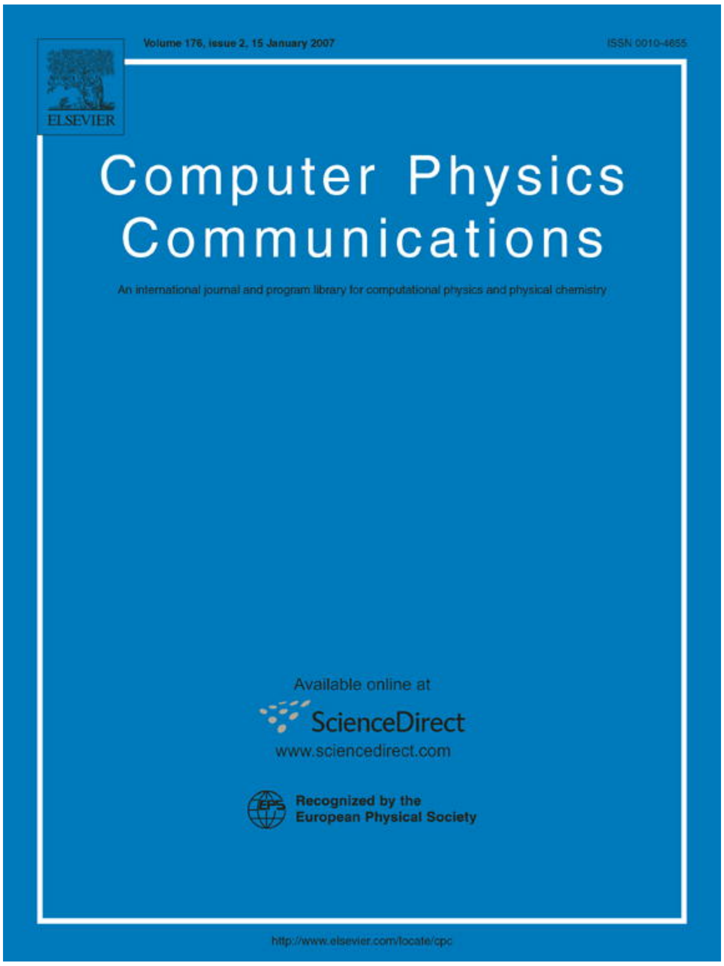
Volume 176, issue 2, 15 January 2007
ISSN 0010-4655
ELSEVIER
Computer Physics Communications
An international journal and program library for computational physics and physical chemistry
Available online at
ScienceDirect
www.sciencedirect.com
Recognized by the European Physical Society
http://www.elsevier.com/locate/cpc

Available online at www.sciencedirect.com
ScienceDirect
Computer Physics Communications 176 (2007) 98–108
Computer Physics Communications
www.elsevier.com/locate/cpc

Stochastic optimization for modeling physiological time series: application to the heart rate response to exercise

M.S. Zakynthinaki *, J.R. Stirling

Departament de Matematiques, Universitat Autonoma de Barcelona, 08193 Bellaterra, Barcelona, Spain

Received 31 March 2006; received in revised form 21 August 2006; accepted 22 August 2006

Available online 16 October 2006

Abstract

Stochastic optimization is applied to the problem of optimizing the fit of a model to the time series of raw physiological (heart rate) data. The physiological response to exercise has been recently modeled as a dynamical system. Fitting the model to a set of raw physiological time series data is, however, not a trivial task. For this reason and in order to calculate the optimal values of the parameters of the model, the present study implements the powerful stochastic optimization method ALOPEX IV, an algorithm that has been proven to be fast, effective and easy to implement. The optimal parameters of the model, calculated by the optimization method for the particular athlete, are very important as they characterize the athlete's current condition. The present study applies the ALOPEX IV stochastic optimization to the modeling of a set of heart rate time series data corresponding to different exercises of constant intensity. An analysis of the optimization algorithm, together with an analytic proof of its convergence (in the absence of noise), is also presented.

PACS: 05.45.Tp; 07.05.Tp; 47.10.Fg; 47.63.Cb; 87.19.Hh

Keywords: ALOPEX stochastic optimization; Modeling; Physiological time series; Heart rate; Nonlinear dynamical systems

1. Introduction

1.1. Stochastic optimization

This work presents the application of stochastic optimization to the calculation of optimal model parameters for physiological data. For the modeling of raw, un-averaged, physiological time series data, the dynamical systems model presented in [1] is used, see Section 1.3 below. The aim of the present work was, as will be described in detail in Section 3, to calculate the optimal values of the model parameters. It is worth noticing here that this is the first time that ALOPEX (*ALgorithm Of Pattern EXtraction*) stochastic optimization has been applied to physiological variables.

For the purposes of the optimization, version IV of ALOPEX stochastic optimization was used. The stochastic optimization algorithm ALOPEX was originally devised in [2,3] for the purpose of experimentally determining receptive fields of individual neurons in the visual pathway. The algorithm of ALOPEX optimization has been studied in detail [4–9] and new versions have been introduced, in addition to the ones already known [4,6]. The particular version of the ALOPEX stochastic optimization used in this study (version ALOPEX IV) has been previously successfully applied [7–9] to the problem of dynamic compensation of atmospheric turbulence. ALOPEX stochastic optimization has been proved to be a very powerful tool for the calculation of the optimal values of the control variables of dynamical systems in real time. The main advantage of the method is that no knowledge of the dynamics of the system or of the functional dependence of the cost function on the control variables, is required. As an optimization algorithm it is very easy in its implementation and is characterized by its effectiveness and speed of convergence in real time.

ALOPEX optimization methods are driven by the parallel incoherent dithering of the control variables and the time dependence of the feedback. Any possible local extrema are avoided

* Corresponding author. Tel.: +34 93 581 1304; fax: +34 93 581 2790.
E-mail addresses: mzakyn@mat.uab.es (M.S. Zakynthinaki), j.r.stirling@mailcity.com (J.R. Stirling).

0010-4655/$ – see front matter © 2006 Elsevier B.V. All rights reserved.
doi:10.1016/j.cpc.2006.08.005

by the introduction of noise. For a brief description of the ALOPEX process we mention the following properties:

- The procedure is iterative. In every iteration the variables that determine the cost function (the control variables) are changed simultaneously by small increments, and the cost function is re-evaluated.
- The changes in a variable depend stochastically on
  - the change of the cost function and
  - the change in that variable over the previous two iterations.
- Since the changes in the control variables accumulate over the iterative process, the current value of each control variable reflects the dependence of the cost function to changes in that variable over all previous iterations.
- The process is guided by two free parameters,
  - the magnitude of the increments of the control variables and
  - the amplitude of noise.

A proof of the convergence of version ALOPEX IV of ALOPEX stochastic optimization algorithm in absence of noise is provided in Section 2, as an indicative convergence behavior of the algorithm.

1.2. Heart rate kinematics in response to exercise

We now provide some physiological background necessary for the present work. As a physiological variable, the heart rate is one of the simplest and most informative of cardiovascular parameters [10–12]. During exercise, an increased heart rate quickly results in an increased blood flow and an increase in the oxygen transported [13]. For constant and sub-maximal exercise intensities the heart rate increases fairly rapidly until it begins to level. This steady state for the heart rate is the optimal heart rate value for meeting the circulatory demands at that specific work rate. The concept of steady state heart rate forms the basis for several tests that have been developed to estimate physical fitness [11].

There are, however, a number of other factors that affect the heart rate, other than exercise intensity. These factors can be the temperature, heat, age, over training, nutrition and hydration, altitude, medication, or infectious disease [10,14,15]. Mental activity is also a very important factor affecting heart rate [14–16]. The authors in [16] emphasize that an accelerated heart rate can be brought about by emotional, as well as physical stress. They also mention that emotional stress is one of the main reasons for heart rate variability in an individual who is at rest. In fact it has been found [17] that during a demanding mental task, the heart rate can be increased by 15%.

For the recording of the heart rate time series data, heart rate monitors are commonly used by athletes, as well as by the general public. There exist numerous popular texts demonstrating the way to analyze and understand the time series recoded with the use of a heart rate monitor, see, for example, [12,14,15,18–20]. Such an analysis can monitor the training intensity measured as a percentage of the maximum heart rate, or measure the training load as the time spent between specific heart rate intervals. The analysis of time series of the heart rate in response to exercise is also commonly used in the field of cardiovascular rehabilitation [21] as well as other areas of health, such as fitness and weight management [22,23]. It is also worth noticing there are also many important clinical applications [24].

Assuming that the heart rate depends on exercise speed (exercise intensity) and time t, let us denote as $s(v,t)$ the function that describes it. The maximum heart rate $s_{\max}$ is the highest heart rate value that can be achieved in an all-out effort to the point of exhaustion. This is a highly reliable value that remains constant for a particular subject [12] and changes only slightly with age (a slight but steady decrease of about one beat per year beginning at 10 to 15 years of age has been observed). The minimum value of the heart rate $s_{\min}$ is the resting value of the heart rate and is dependent on fitness levels. A decrease in the value of $s_{\min}$ indicates an increase in fitness.

Let us now denote as $D(v,t)$ the function describing the heart rate demand of the exercise. For a steady state exercise intensity the value of the demand is the asymptote of the heart rate time series curve. Note that there is always $D(v,t) \geqslant s_{\min}$. For severe or very high intensity exercise, there will be $D(v,t) \geqslant s_{\max}$, which means that the heart rate $s(v,t)$ continues to rise until it reaches $s_{\max}$, assuming the exercise can be continued for a sufficiently long time period [1,25], unless fatigue sets in before $s_{\max}$ can be achieved. When the intensity of the exercise is the minimum possible value for which $s_{\max}$ can be achieved then the demand of the exercise is $D(v,t) = s_{\max}$. For low intensity exercises where the heart rate demand is such that $D(v,t) \ll s_{\max}$, it is believed that the value of the demand, $D(v,t)$, is to a good approximation constant $D(v,t) = D(v)$ and equal to the end of exercise steady state heart rate value, s_{ss}, which can be obtained from the time series of the $s(v,t)$ [1,25]. However, as the intensity of the exercise becomes closer to the absolute velocity limit, the subject will become less efficient, the longer the time of exercise at that intensity [1,26–28]. This could result in a time dependent behavior in the demand $D(v,t)$ [1,25]. Therefore, for higher values of $D(v,t)$ especially for the cases were $D(v,t) \geqslant s_{\max}$ the function $D(v,t)$ is probably a function of time.

1.3. Modeling the response of a physiological variable as a dynamical system

Physiological systems fluctuate in a nonlinear manner, even under resting conditions [29,30]. The data points of beat-to-beat heart rate time series are observed to oscillate around a smooth curve, which describes the basic response pattern, or underlying dynamics [31] of the heart rate response. These oscillations can be the result of noise due to the measuring device or can be physiological, including ectopic beats [32,33], or abnormal breathing during exercise including shallow breathing or breath holding [34].

The modeling and analysis of the time series of physiological responses to exercise is currently a very important area in the field of exercise physiology. From a statistical point of view, the data points are thought to follow a so-called 3-phase model [1,31], which is described as the best fit to the data. It should be noted, however, that before such model is fitted to the physiological time series data, averaging, as a curve smoothing technique, is extensively used. It is worth noticing that, due to the presence of high frequency oscillations in the time series of the raw physiological data, it is only after averaging that the features that are termed the three phases are believed to be observable (for examples regarding modeling the oxygen uptake time series, see [35] and in particular [34], where it is clear that it is impossible to clearly observe three separate phases and time delays in the un-averaged signal). The introduction of different phases and time delays in the time series of single bouts of exercise only serves as an improvement (however marginal) in a process of fitting a particular exponential curve to an averaged data set. Regarding the first two phases, after the combination of the two separate exponentials with a time delay was justified as a statistically better fit to the data, physiological reasons have been sought by the researchers [36–38]. There has been, however, much debate as to the physiological reasons for the third phase, the so-called slow component [39–41] although many mechanisms underlying its existence have been refuted. It can be concluded therefore that the existence of three different phases and time delays is highly debatable, from both a physiological and a mathematical point of view, see also [1].

It should be noted here that, as far as the oxygen uptake kinetics is concerned, modifications of the 3-phase model have been suggested, such that phase 3 (the slow component) is modeled not as a mono-exponential, but consists of a number of exponential components to account for the possible recruitment of additional motor units. The authors in [42] presented a 10-compartment model as an example. Other findings in the same field of exercise physiology conclude that it is more plausible that phase 3 is composed of progressive increases in the oxygen uptake, rather than being a single and abrupt increase in oxygen demand, as this way the model would be more consistent with a dynamic maintenance of energy balance [43]. These findings suggest that the so-called slow component of the oxygen uptake kinetics should not be modeled as a single mono-exponential event but can develop in serial increments during prolonged heavy exercise. The model suggested in [42] used a sequence of increments, which become smaller and smaller in an effort to follow the underlying response pattern, refers to the way a smooth function is approximated using first principles of infinitesimal calculus. It becomes obvious therefore that the conclusion of such thinking is that the physiological data should be modeled using a smooth function describing the kinetics of the physiological variables $s(t)$.

As no conclusive physiological reason has been provided by the researchers in the field of exercise physiology for the existence of time delays and separate phases (other than data fitting of averaged data sets) we use a model given by smooth function that will describe the underlying dynamics of the response to exercise [1]. It should be noted that the model in [1] is built from the basic underlying physiological principles and, unlike the 3-phase model, is not a curve fitting technique.

The dynamical systems model presented in [1], which describes the kinetics of the oxygen uptake, can be appropriately modified to describe the kinetics of the heart rate response to exercise [10,25]. It is worth noticing here that the process of optimization of the model parameters described in the present study can be successfully applied to both models of oxygen uptake and heart rate kinetics. To give a brief description of the model [1,10,25], let us assume that $s(v,t)$ represents the physiological variable which depends on the velocity of the exercise v and the time t (see Section 1.2). The model is expressed as a set of coupled ordinary differential equations of the form

$$\dot{s}(v,t) = \tilde{A}\big[s(v,t) - s_{\min}\big]^B \big[s_{\max} - s(v,t)\big]^C \times \big[D(v,t) - s(v,t)\big]^E, \tag{1}$$

$$\dot{v} = I(t), \tag{2}$$

where $s_{\min} \leqslant s(v,t) \leqslant s_{\max}$.

The model described by Eqs. (1) and (2) [1,10,25] is based on the fact that the rate of increase in the value of the physiological variable, $\dot{s}(v,t)$, goes to zero on three specific occasions: (a) when $s = s_{\min}$, (b) when $s = s_{\max}$ and (c) when $s = D(v,t)$ for $s_{\min} \leqslant D(v,t) \leqslant s_{\max}$. Note that if $D(v,t) \geqslant s_{\max}$ then $\dot{s}(v,t) = 0$ when $s = s_{\max}$. The vector $\dot{v} = I(t)$ defines the rate of change of exercise intensity. For linear exercise intensities there is $\dot{v} = c$ where c is a constant; the case $c = 0$ refers to the case of steady state exercise.

The model described by Eqs. (1) and (2) is able to deal with exercise intensities that might not be constant (i.e. that can be functions of time). The present study, however, focuses on the simple case where $\dot{v} = 0$ (which refers to a steady state exercise), as this is the case where the heart rate demand is known, especially for low exercise intensities, as is described in Section 1.2. In addition, this case of constant exercise intensity is of much practical importance, as almost all of the current testing methods used in exercise physiology are based on the body's response to constant exercise intensity. It should be noted here that the heart rate response to non constant exercise intensities is far more complicated due to the presence of nonlinearities and coupling between other variables in the body. As a result there is very little basic physiological knowledge in this area. However, to understand the heart rate response to an exercise intensity which is a function of time, the response to the constant exercise intensity should be first studied and understood.

Let us now give a brief description of the positive parameters $\tilde{A}, B, C$ and E which control the shape of the curve that models the kinetics of the physiological variable $s(v,t)$ [25]. As can be observed from Eq. (1), parameter $\tilde{A}$ controls the overall rate of change of $s(v,t)$. Parameter B controls the dynamics in the neighborhood of the minimum value $s_{\min}$ and similarly, parameter C controls the dynamics in the neighborhood of the maximum value $s_{\max}$. The parameter E controls the dynamics in the neighborhood of the demand $D(v,t)$. We note that, assuming that the variable $s(v,t)$ is expressed in beats/min, the parameters B, C and E in Eq. (1) are dimensionless, whilst parameter $\tilde{A}$ has dimensions of $(\text{beats/min})^{1-B-C-E}\ \text{min}^{-1}$. When the model is fit to the time series of physiological data of a particular athlete, the values of the model parameters are very important as they characterize the athletes current condition, across the continuum of possible exercise intensities. Changes in the parameters indicate changes in the current fitness level of that particular athlete.

Without loss of generality and for simplicity and numerical reasons, the variable $s(v,t)$ in Eq. (1) can be replaced [25] by the dimensionless normalized variable

$$\tilde{s}(v,t) \equiv \frac{s(v,t) - s_{\min}}{s_{\max} - s_{\min}}$$

so that $0 \leqslant \tilde{s}(v,t) \leqslant 1$. This way the demand of the exercise $D(v,t)$ is also normalized,

$$\tilde{D}(v,t) \equiv \frac{D(v,t) - s_{\min}}{s_{\max} - s_{\min}}.$$

According to Section 1.2, there is $\tilde{D}(v,t) \geqslant 1$ for values of severe or very high exercise intensity and $\tilde{D}(v,t) = 1$ when the exercise velocity is the minimum possible value for which $\tilde{s}(v,t) = \tilde{s}_{\max} = 1$ can be reached. For exercise intensities where the heart rate demand is such that $\tilde{D}(v,t) \ll 1$, the value of the exercise demand is approximately constant and equal to the end of exercise steady state, where $\tilde{s}_{ss} < 1$ (see Section 1.2). For simplicity in what follows, the normalized demand $\tilde{D}(v,t)$ will be denoted simply as $D(v,t)$ and similarly the normalized variable $\tilde{s}(v,t)$ will be simply denoted as $s(v,t)$.

Taking the above into account, the dynamics of the dimensionless normalized heart rate variable $s(v,t)$, where $0 \leqslant s(v,t) \leqslant 1$, will be described by the following system of equations (see also [25,44]):

$$\dot{s}(v,t) = A\big[s(v,t)\big]^B\big[1 - s(v,t)\big]^C\big[D(v,t) - s(v,t)\big]^E, \quad (3)$$

$$\dot{v} = I(t), \quad (4)$$

where A is the dimensionless parameter $A = \tilde{A}(s_{\max} - s_{\min})^{B+C+E-1}$.

The optimal values of the parameters A, B, C and E of the model described by Eqs. (3) and (4) are calculated, in the present study, by use of ALOPEX IV stochastic optimization (see Section 1.1, as well as Section 2). These values are such that the fit of the curve provided by integration of Eqs. (3) and (4) to the curve that describes the basic response pattern of the data (which is derived though Fourier low-pass filtering) is optimal, see Section 3.2.

2. ALOPEX IV stochastic optimization

In what follows we will give a general detailed description of the optimization method, as well as a proof of its convergence. Let us assume that the function $f \equiv f(x_1, x_2, \ldots, x_N; y_1, y_2, \ldots, y_M)$ denotes the cost function, i.e. it is the function that describes the system, the performance of which we want to optimize. In general, function f depends on the set of N parameters $x_1, x_2, \ldots, x_N$, that are the control variables, as well as the set of M parameters $y_1, y_2, \ldots, y_M$, that are not under control, and may be internal or external parameters of the system. The aim of the optimization is to find the (optimum) values of the control variables that maximize function $f(x_1, x_2, \ldots, x_N; y_1, y_2, \ldots, y_M)$. Since the parameters $y_1, y_2, \ldots, y_M$ are not under control in what follows f will be treated as a function of the set of the control variables $x_1, x_2, \ldots, x_N$ only, i.e. $f \equiv f(x_1, x_2, \ldots, x_N) = f(\vec{x})$,

$$\vec{x} = \begin{bmatrix} x_1 \\ \vdots \\ x_N \end{bmatrix} \in \mathbb{R}^N.$$

Let $x_i^{(k)}$ be the value of the ith control variable after the kth iteration and let $f^{(k)}(x_1^{(k)}, x_2^{(k)}, \ldots, x_N^{(k)})$ be the value of the control function after the kth iteration. According to the version IV of the ALOPEX stochastic optimization algorithm first presented and tested in [7–9], the value of the ith control variable is evaluated, at each iteration, according to the rule:

$$x_i^{(k+1)} = x_i^{(k)} + c\Delta x_i{}^{(k)} \frac{\Delta f^{(k)}}{|\Delta f^{(k-1)}|} + g_i^{(k)}, \quad i = 1, \ldots, N, \quad (5)$$

where

$$\Delta x_i^{(k)} \equiv x_i^{(k)} - x_i^{(k-1)},$$
$$\Delta f^{(k)} \equiv f^{(k)} - f^{(k-1)},$$

and

$$\Delta f^{(k-1)} \equiv f^{(k-1)} - f^{(k-2)}.$$

In the absence of noise the algorithm (5) is one-dimensional, since the vectors $\Delta x_i^{(k)}$ and $\Delta x_i^{(k+1)}$ are co-linear. The noise terms g_i are therefore essential ingredients in the process, as they provide the agitation necessary to drive the process and to overcome local extrema [2,4,6–9,45]. The dynamics of the process depends strongly on the mean amplitude of the g_i terms.

As can be observed, this version of ALOPEX uses information of the previous two steps of the optimization process, through the factor $|\Delta f^{(k-1)}|$ by which the difference $\Delta f^{(k)}$ is divided. This factor also acts as a normalization parameter, as the value of $\frac{\Delta f^{(k)}}{|\Delta f^{(k-1)}|}$ has the same value range, regardless of the choice of the cost function. The sign of the difference $\Delta f^{(k)}$ drives the process, according to the principles of the ALOPEX optimization method [2,4,6–9,45].

The convergence of ALOPEX III in the absence of noise has been proven analytically in [4]. An analytic proof of the convergence of version IV of the algorithm has not been presented, however, even though the particular version of the algorithm has been tested and the results of its successful implementation have been presented, see [7–9]. In the following we include a proof of the convergence of ALOPEX IV in the absence of noise, following similar steps as in [4], calculating also analytically the optimal value of constant c of Eq. (5).

Assuming that $f(\vec{x})$ is a twice differentiable in $\mathbb{R}^N$, i.e. $f \in C^2(\mathbb{R}^N)$, its second order Taylor expansion is given by

$$f(\vec{x} + \vec{h}) \approx f(\vec{x}) + \vec{G}^{\mathrm{T}}\vec{h} + \frac{1}{2}\vec{h}^{\mathrm{T}} H \vec{h}, \quad (6)$$

where $\vec{G}$ is the gradient vector of f at $\vec{x}$ and H is the Hessian matrix of f at $\vec{x}$, defined respectively as

$$\vec{G} = \begin{bmatrix} \frac{\partial f}{\partial x_1} \\ \vdots \\ \frac{\partial f}{\partial x_N} \end{bmatrix}, \qquad H = \begin{bmatrix} \frac{\partial^2 f}{\partial^2 x_1} & \cdots & \frac{\partial^2 f}{\partial x_1 \partial x_N} \\ \vdots & & \vdots \\ \frac{\partial^2 f}{\partial x_1 \partial x_N} & \cdots & \frac{\partial^2 f}{\partial^2 x_N} \end{bmatrix}.$$

Lemma 1. *Let $f(\vec{x}) \in C^2(\mathbb{R}^N)$. If the Hessian matrix of f at $\vec{x}$ is negative-definite, i.e. if*

$$\vec{x}^{\mathrm{T}} H \vec{x} < 0 \quad \forall \vec{x} \in \mathbb{R}^N,$$

then the value

$$\hat{c}_k = -\frac{\vec{G}_k^{\mathrm{T}} \Delta \vec{x}_k}{\Delta \vec{x}_k^{\mathrm{T}} H \Delta \vec{x}_k} \frac{|\Delta f^{(k-1)}|}{\Delta f^{(k)}}$$

maximizes the value of the function f at

$$\vec{x}_{k+1}(c_k) = \vec{x}_{k+1} = \vec{x}_k + c_k \frac{\Delta f^{(k)}}{|\Delta f^{(k-1)}|} \Delta \vec{x}_k, \tag{7}$$

where $\vec{x}_k \equiv [x_1^{(k)}, \ldots, x_N^{(k)}]^{\mathrm{T}}$.

Proof. By setting

$$\vec{h}_k \equiv \frac{\Delta f^{(k)}}{|\Delta f^{(k-1)}|} \Delta \vec{x}_k,$$

relation (7) becomes

$$\vec{x}_{k+1} = \vec{x}_k + c_k \vec{h}_k \tag{8}$$

and the constant c_k is to be chosen so as to maximize $f^{(k+1)} \equiv f(\vec{x}_{k+1})$ on an interval of the line that passes through $\vec{x}_k$ in the direction of $\vec{h}_k$.

The combination of Eqs. (6) and (8) gives

$$W(c_k) \equiv f(\vec{x}_{k+1}) - f(\vec{x}_k) = c_k \vec{G}_k^{\mathrm{T}} \vec{h}_k + \frac{c_k^2}{2} \vec{h}_k^{\mathrm{T}} H \vec{h}_k. \tag{9}$$

Function $W(c_k)$ has an extremum at the point where $dW/dc_k = 0$. The corresponding value of $c_k \equiv \hat{c}_k$ is

$$\hat{c}_k = -\frac{\vec{G}_k^{\mathrm{T}} \vec{h}_k}{\vec{h}_k^{\mathrm{T}} H \vec{h}_k}$$

or, equivalently,

$$\hat{c}_k = -\frac{\vec{G}_k^{\mathrm{T}} \Delta \vec{x}_k}{\Delta \vec{x}_k^{\mathrm{T}} H \Delta \vec{x}_k} \frac{|\Delta f^{(k-1)}|}{\Delta f^{(k)}}. \tag{10}$$

It is therefore evident that whenever H is negative definite, the value of $\hat{c}_k$ in (10) is a maximizer, since

$$W(\hat{c}_k) = -\frac{(\vec{G}_k^{\mathrm{T}} \Delta \vec{x}_k)^2}{2 \Delta \vec{x}_k^{\mathrm{T}} H \Delta \vec{x}_k} \geqslant 0. \tag{11}$$

This completes the proof. □

It should be noted here that the assumption $f(\vec{x}) \in C^2(\mathbb{R}^N)$ of Lemma 1 is equivalent to f being strictly concave. This assumption can be very often relaxed to hold only in a neighborhood of the maximum.

To prove the convergence of ALOPEX IV algorithm, in the absence of noise, we follow a way similar to the one used to prove the convergence of ALOPEX III [4]. We will make use of the concept of the energy inner product and the energy norm corresponding to a negative-definite matrix, defined for $\vec{x}, \vec{y} \in \mathbb{R}^N$ as

$$(\vec{x}, \vec{y})_H = -\vec{x}^{\mathrm{T}} H \vec{y}$$

and

$$\|\vec{x}\|_H = (\vec{x}, \vec{x})_H^{1/2} = \left(-\vec{x}^{\mathrm{T}} H \vec{x}\right)^{1/2},$$

respectively. We also define the Energy $E(\vec{x})$ of the system to be the quantity

$$E(\vec{x}) = \|\vec{x}\|_H^2 = -\vec{x}^{\mathrm{T}} H \vec{x}.$$

Proposition 1. *Consider the ALOPEX IV process (Eq. (7)) in the absence of noise, that is*

$$x_i^{(k+1)} = x_i^{(k)} + c \Delta x_i^{(k)} \frac{\Delta f^{(k)}}{|\Delta f^{(k-1)}|}, \quad i = 1, \ldots, N. \tag{12}$$

Under the hypothesis that the Hessian matrix H is negative-definite, if we set

$$c = \hat{c}_k,$$

where $\hat{c}_k$ is as defined in Lemma 1, the process in (12) converges in the sense that

$$\|\vec{x}_{k+1} - \vec{x}_{\mathrm{opt}}\|_H \leqslant \|\vec{x}_k - \vec{x}_{\mathrm{opt}}\|_H, \tag{13}$$

where $\vec{x}_{\mathrm{opt}}$ is a maximizer of the function $f(\vec{x})$.

Proof. Recalling the Taylor expansion in (6) and observing that $\vec{G}(\vec{x}_{\mathrm{opt}}) = \vec{0}$, then in the neighborhood of $\vec{x}_{\mathrm{opt}}$ there is

$$f(\vec{x}) - f(\vec{x}_{\mathrm{opt}}) = \frac{1}{2} (\vec{x} - \vec{x}_{\mathrm{opt}})^{\mathrm{T}} H (\vec{x} - \vec{x}_{\mathrm{opt}}),$$

and

$$E(\vec{x} - \vec{x}_{\mathrm{opt}}) = -2\left[f(\vec{x}) - f(\vec{x}_{\mathrm{opt}})\right].$$

A combination of the above equations and Eqs. (9) and (11) yields

$$E(\vec{x}_k - \vec{x}_{\mathrm{opt}}) \geqslant E(\vec{x}_{k+1} - \vec{x}_{\mathrm{opt}})$$

which in turn leads to the relation

$$\|\vec{x}_{k+1} - \vec{x}_{\mathrm{opt}}\|_H \leqslant \|\vec{x}_k - \vec{x}_{\mathrm{opt}}\|_H$$

completing the proof. □

3. Beat-to-beat heart rate time series: curve smoothing and model fitting

3.1. Fourier low-pass filtering of the heart rate time series

Assuming the sequence $\{s_k\}_{k=0}^{N-1}$ of the N data points, its discrete Fourier transform $\{S_n\}_{n=0}^{N-1}$ can be computed in $\mathrm{O}(N \log_2 N)$ operations by use of the Fast Fourier Transform algorithm (FFT). For the purposes of the present study the FFT algorithm was adopted from [46]. When N is not an integer power of 2, as is the general case of physiological data, the length of the time series can be artificially increased by adding zero values, a method that is referred to as zero-padding [46]. It is worth noticing here that, in order to avoid any oscillatory effects (Gibb's phenomenon) in the time series of the filtered data [47,48], a smooth transition that does not contain abrupt discontinuities but decays to zero gradually was implemented between the pass-band of frequencies and the stop-band [46].

Let now $\{S_n^f\}_{n=0}^{N-1}$ denote the set of frequency points after the application of the filter. The inverse FFT of the points $\{S_n^f\}_{n=0}^{N-1}$ results in the calculation of the time series $\{s_k^f\}_{k=0}^{N-1}$, which forms a smooth curve describing the basic response pattern of the heart rate data.

3.2. Fitting the model to the basic response pattern of the data

Assuming that the parameters A, B, C and E of Eqs. (1) and (2) are known and so is the function $D(v,t)$ that describes the demand, Eqs. (1) and (2) can be integrated in respect to time to give the time series $\{s_k^m\}_{k=0}^{N-1}$ that model the response of the physiological variable s (heart rate). As mentioned before, for numerical simplicity, in the sections that follow the modeling process will be assumed to be described by Eqs. (3) and (4), which describe the dynamics of the normalized variable $0 \leqslant s(v,t) \leqslant 1$.

As described in Section 3.1, the time series $\{s_k^f\}_{k=0}^{N-1}$ describe the smooth curve of the response pattern of the data. For each point $k = 0, \ldots, N-1$ the sum of the vertical distances (residuals R) between the smooth curve describing the data and the curve provided by the model is given as follows,

$$R = \sum_{k=0}^{N-1} \left(s_k^f - s_k^m\right)^2.$$

Following the above considerations, the curve $\{s_k^m\}_{k=0}^{N-1}$ provided by the model would be considered to be an optimal fit to the smoothed data curve $\{s_k^f\}_{k=0}^{N-1}$ if the value of R is minimum. The process of optimizing the fit of the model to the data curve can be then thought to be equivalent to the process of maximizing the cost function f of the system (see Section 2), where we define

$$f \equiv -R = \sum_{k=0}^{N-1} \left(s_k^f - s_k^m\right)^2. \tag{14}$$

4. Raw data recording and editing

A healthy male subject (age 33, height 1.83 m and weight 82 kg) served as the test subject. The subject's heart rate parameters were: maximum heart rate $s_{\max} = 185$ beats/min, minimum heart rate $s_{\max} = 40$ beats/min. The subject preformed a set of constant intensity exercises followed by a 10 minute static recovery period, during which the subject lay horizontally and still on the floor. The experiment was carried out on a tartan track. As can be seen in Table 1, the set of exercises followed a square wave protocol consisting of five work periods of four laps each with a velocity of $v_1 = 13.4$ km/h, $v_2 = 14.4$ km/h, $v_3 = 15.7$ km/h, $v_4 = 17.0$ km/h and $v_5 = 17.9$ km/h, respectively. The velocity of each exercise was assured to be constant by assuring constant 50 m times; its values were measured with the traditional way (recording the time for each 400 m lap) as well as with the use of a Garmin Forerunner 201 GPS system [49] and a Polar S625x speed-distance heart rate monitor [32].

Table 1
Corresponding velocities of the data sets

Data set	Velocity
1 on-transient	$v_{1_{\text{on}}} = 13.4$ km/h
1 off-transient	$v_{1_{\text{off}}} = 0.0$ km/h
2 on-transient	$v_{2_{\text{on}}} = 14.4$ km/h
2 off-transient	$v_{2_{\text{off}}} = 0.0$ km/h
3 on-transient	$v_{3_{\text{on}}} = 15.7$ km/h
3 off-transient	$v_{3_{\text{off}}} = 0.0$ km/h
4 on-transient	$v_{4_{\text{on}}} = 17.0$ km/h
4 off-transient	$v_{4_{\text{off}}} = 0.0$ km/h
5 on-transient	$v_{5_{\text{on}}} = 17.9$ km/h
5 off-transient	$v_{5_{\text{off}}} = 0.0$ km/h

It should be noted here that a set of physiological time series data is characterized as on-transient (see Table 1) when the kinetics of the physiological variable is following an increase in the demand. In other words, for the data presented in Table 1, the on-transient parts of the data sets are the parts which correspond to the heart rate kinetics in response to an exercise of nonzero velocity. Similarly, the kinetics that follows a decrease in the demand is characterized as off-transient. In the present data sets the off-transient parts correspond to the heart rate kinetics in response to zero velocity (the recovering period with the subject lying on the floor).

The heart rate data were recorded in a beat-to-beat basis using a Polar S810i heart rate monitor [33]. It should be noted here that heart rate monitors have the big advantage that they are portable and can be used for recordings in the field, whilst they also have been shown to provide reliable measurements of the electrocardiogram (ECG), when compared with direct ECG measurements [50–52]. It is worth noticing that, due to the fact that any external electromagnetic fields can disturb the beat-to-beat heart rate recording, care was taken to ensure that the environment that the experiments took place was free of any additional electromagnetic signals (such as high tension power lines, engines producing electromagnetic fields, mobile phones, etc.).

Following the notation of Section 3.1, the raw recorded heart rate data sets consist of the sequence of N data points $\{s_k\}_{k=0}^{N-1}$. The only editing performed on the points $\{s_k\}_{k=0}^{N-1}$ of each data set was to exclude occasional errant data points. The reason for such occasional deviations from the local mean heart rate can be either technical, physiological, or can be ectopic beats which can occur sporadically due to abnormal origin. Studies can be found in the literature in which the data is edited by omitting any points with values greater than 6 standard deviations from the local mean value [53–55]. In the present study, however, any

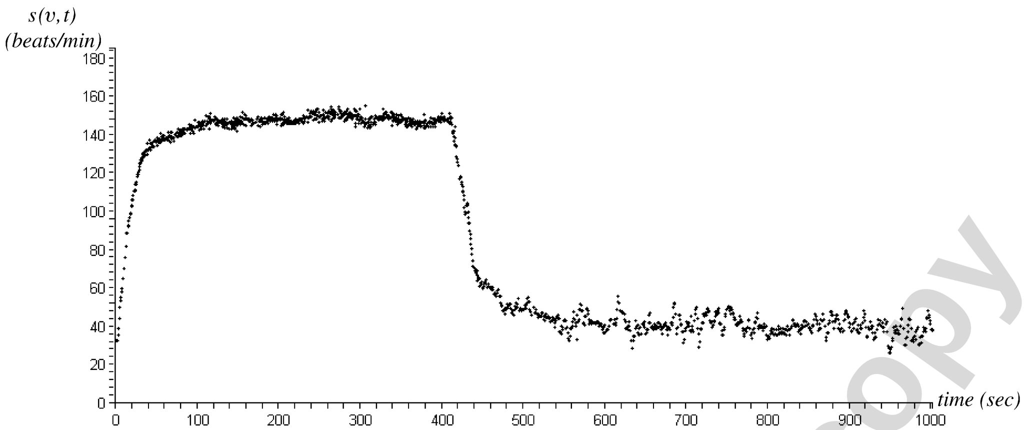

Fig. 1. Raw data set corresponding to exercise 2: The duration of the on-transient (velocity $v_{2_{\text{on}}} = 14.4$ km/h) was 402 s and the duration of the off-transient 600 s.

abnormal data points which very rarely appeared in the time series data were excluded when their values were larger than 10 standard deviations from the local mean heart rate. The abnormal values of occasional data points that occurred mainly due to technical reasons, such as sporadically missed R waves (resulting in a HR interval about two times longer than the normal one), misread T waves (resulting in a sudden too short HR interval), or recorded spurious peak waves instead of the R waves (resulting in a pair of too short and too long intervals) were appropriately restored to their proper values depending on the cause of the measurement error.

In Fig. 1 we present as an example of the data, the on- and off-transient parts of the second data set. The duration of the on-transient exercise was 402 s with a velocity a $v_{2_{\text{on}}}$ and the estimated demand of the exercise 156 beats/min. The heart rate oscillations that can be observed mostly in the off-transient part of the data can be explained if we take into account (see Section 1.2) the other factors affecting the heart rate, such as emotional stress [16,17] due to distractions during the recovery.

5. Numerical implementation

5.1. The demand of each exercise set

As described in Section 4, the present study focuses on modeling the kinetics of the heart rate in response to steady state exercise, i.e. the case where $\dot{v} = 0$. In this case and for sufficiently low exercise intensities, it can be assumed that there is also $\dot{D}(v,t) = 0$, i.e. the demand is not a function of time but depends only on the exercise velocity v, therefore there is $D(v,t) = D(v)$, see Sections 1.2 and 1.3. Assuming now a particular data set that corresponds to an on-transient exercise of a low intensity of a constant velocity v, the demand $D(v)$ is, as mentioned in Section 1.3, a constant and its value $D < 1$ characterizes the intensity of this particular data set. The value of the demand D for a particular velocity can be observed from the time series of the data: as mentioned in Section 1.2, for such steady state exercise intensities the value of the demand can be given by the asymptote of the heart rate time series curve. Table 2 shows the estimated values of the demand, for each data set of the present study.

Table 2
Estimated demands of the data sets

Data set	Estimated $D(v)$ (normalized)
1 on-transient	0.730
1 off-transient	0.150
2 on-transient	0.800
2 off-transient	0.220
3 on-transient	0.870
3 off-transient	0.220
4 on-transient	0.935
4 off-transient	non constant
5 on-transient	0.940
5 off-transient	non constant

As can be observed in Table 2, the values of the demand $D(v)$ for the on-transient data sets can be estimated, to a good approximation, to be constant, as the exercise intensity was not sufficiently heavy to induce a time dependent demand (see Section 1.3). However, regarding the demand of the off-transient kinetics, when the preceding on-transient exercise intensity is heavy then we believe that the demand of the following off-transient is not a constant function of time, especially in the initial stages of the off-transient. This belief is backed up by our analysis of the off-transient kinetics data, for the two heaviest exercise intensities. As mentioned in Section 1.2, the heart rate is affected by many parameters other that the exercise intensity. As some of these parameters play an important role in the off-transients that follow a high intensity exercise, the demands of these off-transients can no more be considered constant.

5.2. The optimization variables and parameters

For the purposes of the present study, the cost function f of the system is the one defined by Eq. (14) and, as was described in Section 3.2, refers to the sum of the residuals between the smooth curve describing the data and the curve provided by the model (Eqs. (3) and (4)). As the demand D that describes a particular exercise can be assumed to be constant (except the cases mentioned above) the cost function f of the system can

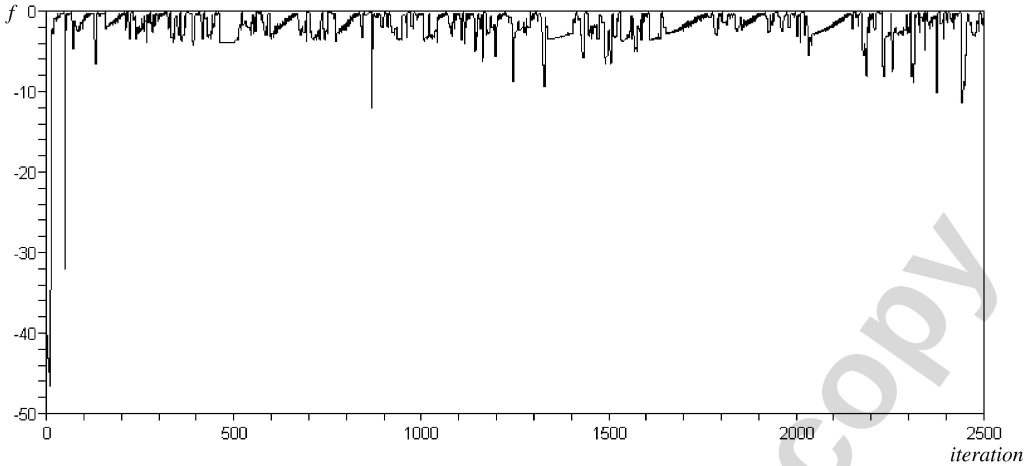

Fig. 2. A typical optimization run. The data correspond to the on-transient data set of exercise 2 (velocity $v_{2_{on}} = 14.4$ km/h).

be thought to be a function of the parameters A, B, C and E of the model.

The aim of the optimization is to achieve an optimum fit of the curve provided by the model (Eqs. (3) and (4)) by the maximization of the cost function f, as described by Eq. (14). This is achieved via appropriately modifying the shape of the curve provided by the model, i.e. via the appropriate changes in the values of the control variables A, B, C and E. It should be noted here that, in accordance with the results of the analysis of the model presented in [1,25,44], the value of the parameter E was kept constant and equal to $E = 1$ during the modeling and optimization process. Therefore in the case of the present study, the number of the control variables N (Eq. (7)) of the optimization process described in the present study was $N = 3$, and $f \equiv f(A, B, C)$.

We should point out here that the principles of exercise physiology put a constrain regarding the optimum value of the parameter C, which follows from the linear stability analysis of the model presented in [25]. For the model of Eqs. (3) and (4), in the present case of $B \neq 1$, $C \neq 1$ and $E = 1$, the eigenvalue that controls the attractor $s(t) = D$ is given by the expression [25]

$$\lambda = -AD^B(1 - D)^C. \tag{15}$$

For values of demand $0 < D < 1$ the eigenvalue λ is negative and the solution at $s(t) = D$ is therefore attracting, since $A > 0$. However for exercises of higher intensities where there is $D > 1$ the eigenvalue becomes a complex number, the real part of which is required to be negative, for the solution to be attracting at $s(t) = D$. Since the real part of $(1 - D)^C$ for $D > 1$ is $(D - 1)^C \cos(C\pi)$ then the optimal calculated values of parameter C have to be such that $\cos(C\pi) > 0$, see also [44].

Regarding the numerical value of constant c_k of the optimization algorithm (Eq. (10) in Section 2), this was found to be always inside the interval [0, 1]. This allowed us to consider c_k constant from the beginning of the optimizing process, as described in Eq. (7), with a value $0 < c < 1$, see also [8]. We note that, for the results presented in the present paper, the value of c was kept constant at $c = 0.1$, a value that was found to be the optimal by trial and error. The optimal mean value of the noise terms $g_i^{(k)}$ was also found by trial and error to be approximately equal to 0.01% of the values of the control variables $x_i^{(k)}$.

5.3. Results

5.3.1. A typical performance of the algorithm

Fig. 2 presents a typical run of 2500 iterations of the optimization process. The cost function under optimization in Fig. 2 was the one corresponding to the on-transient (velocity $v_{2_{on}}$) data set of exercise 2 (see Fig. 1). The satisfactory performance of the optimization algorithm can be easily observed. The method is able to reach the neighborhood of the optimal parameter values within the fast time of 14 iterations, despite the fact that the process starts from a very low value of the cost function f (the initial choice of the model parameters A, B and C provide a very bad fit to the data). Although the characteristic 'jumps' of the version IV of ALOPEX, see [8], can also be observed in Fig. 2, they are of minor importance, as the method is able to keep the value of the cost function within its maximum levels throughout the large number of iterations.

5.3.2. Optimal model parameter values

The optimization method of ALOPEX IV was applied to all constant demand data sets. As can be seen in Table 1, these are the data sets corresponding to the on-transient data of all exercises 1, 2, 3, 4 and 5 and the off-transient data corresponding to the low intensity exercises 1, 2 and 3. A run of 10000 iterations of ALOPEX IV optimization provided, for each exercise, a list of parameter combinations $\{A, B, C\}$ that provided optimal fit of the model of Eqs. (3) and (4) to each data set. As described in the sections above, during the optimization process the parameter E was kept constant $E = 1$ and so was the parameter D of the demand, the value of which, for each on- and off-transient data set can be found in Table 2. The criterion for choosing the optimal sets of parameters $\{A, B, C\}$ was that these parameters should provide an optimal (maximum) value of the cost function.

Fig. 3 presents a three-dimensional graph of these optimal parameter sets, for all the constant demand exercises of Table 1.

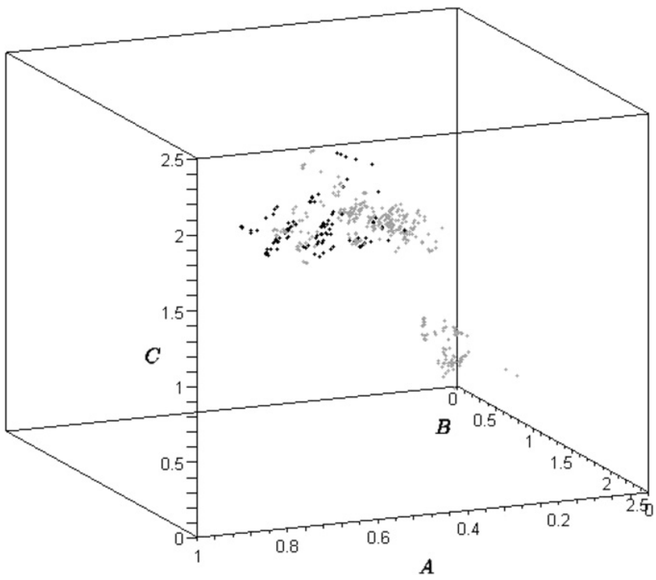

Fig. 3. Three-dimensional view of the optimal combinations of the values of the parameters A, B and C. Grey points: optimal model fit for all the on- and off-transient data sets of the low intensity exercises, black points: optimal model fit for the on-transients of the high intensity exercises 4 and 5.

Every optimal combination of the parameters $\{A, B, C\}$ is represented as a point in the three-dimensional space of A, B and C. It is worth noticing that a realistic range of the model parameter values is $0 \leqslant A \leqslant 1.0$, $0 \leqslant B \leqslant 2.5$ and $0 \leqslant C \leqslant 2.5$ (the constrain in the values of C, $\cos(C\pi) > 0$, as described in Section 5.2, was also taken into account). In Fig. 3 the grey points correspond to all the on- and the off-transient data sets of the low intensity exercises, while the black points are the optimal parameter combinations for the on-transients of the high intensity exercises 4 and 5.

Observation of Fig. 3 verifies the theoretical criterion [1, 25] that the parameter combinations that provide a best fit to the exercise data are characteristic of the athlete's current condition of fitness (see also Section 1.3) and, for a curve that models a constant demand exercise, have the same values regardless the exercise intensity. In particular, in Fig. 3, clusters of optimal parameter values can be observed, leading to the conclusion that the combination of optimal parameter values that characterize a subject can be found in an 'optimal parameter neighborhood'. It is worth pointing out that, as can be seen in Fig. 3, the parameter combinations that best fit the low intensity exercises (grey points) form two separate clusters in the three-dimensional space of A, B, C. It can also be observed, however, that the points of the optimal parameter values for the high intensity exercises (black points in Fig. 3) can only be found inside the 'big' parameter cluster. A two-dimensional view of the optimal parameter combinations can been found in Fig. 4.

It should be noticed here that, due to experimental noise, the optimal parameter clusters of each exercise has a slightly different shape, size and place, in the three-dimensional space of A, B, C. This should be of course expected as we are dealing with raw experimental data. The optimal parameter combinations that characterize the particular subject for all exercise intensities, are therefore assumed to be the common parameter combinations of all optimal sets, i.e. the parameter combinations that lie within the intersection of all optimal clusters. Careful observation of the numerics of the optimization results reveals that the intersection of all sets is the small parameter neighborhood

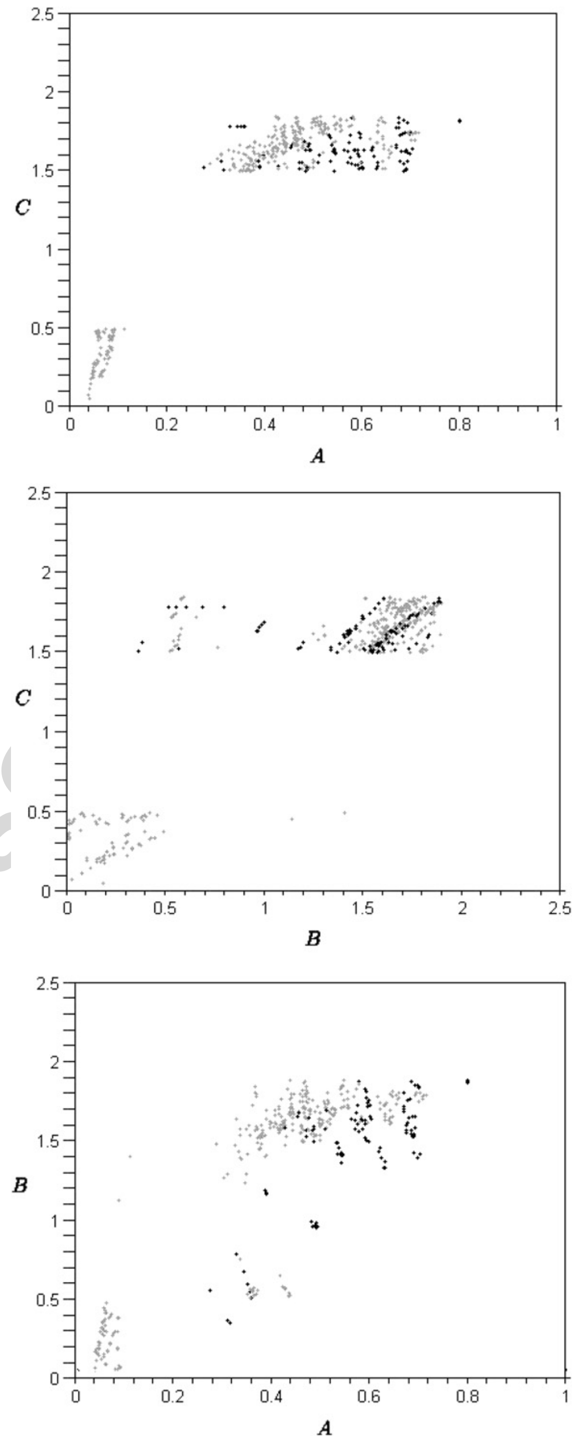

Fig. 4. Two-dimensional views of the optimal combinations of the values of the parameters A, B and C. Grey points: optimal model fit for all the on- and off-transient data sets of the low intensity exercises, black points: optimal model fit for the on-transients of the high intensity exercises 4 and 5.

$$0.45 < A < 0.65, \quad 1.55 < B < 1.75, \quad 1.60 < C < 1.80.$$

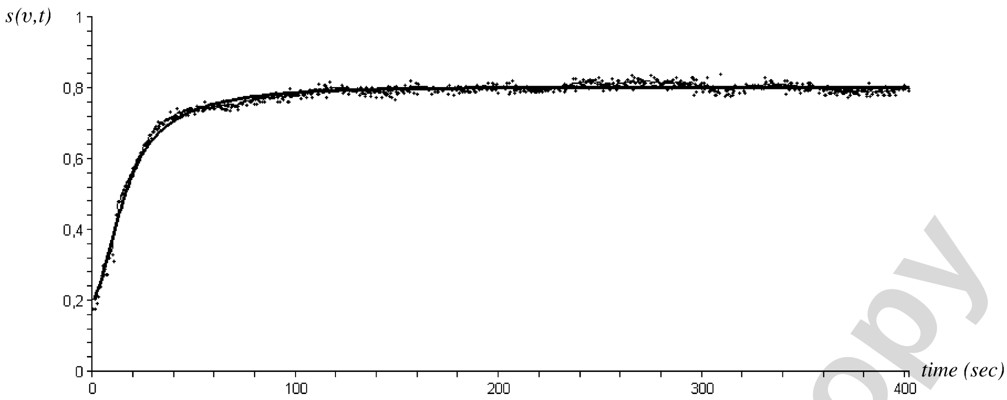

Fig. 5. Optimal model fit to the on-transient data points of Fig. 1. Thick line: model, thin line: Fourier low-pass curve.

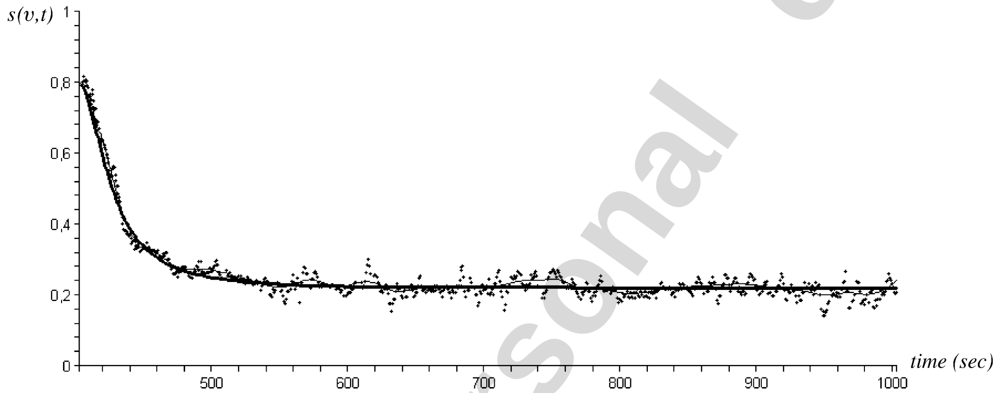

Fig. 6. Optimal model fit to the off-transient data points of Fig. 1. Thick line: model, thin line: Fourier low-pass curve.

A combination of the parameter values above is, therefore, characteristic of the particular subject and its current fitness condition.

5.3.3. An example of optimal model fit

Figs. 5 and 6 present, as an example of the performance of the optimization method, an optimum model fit (thick curve) to the raw data of Fig. 1 which corresponds to the data set of exercise 2. In these figures, the smooth curve describing the basic response pattern of the data points, which is calculated through low-pass Fourier filtering, can also be seen (thin curve). The values of the model parameters used for the fit of Figs. 5 and 6 were, $A = 0.54$, $B = 1.63$, $C = 1.75$ (recall that $E = 1.0$, $D = 0.8$ for the particular on-transient data set and $D = 0.22$ for the off-transient data set of exercise 2, see Section 4). It is worth noticing here that, as mentioned in the previous section, the particular optimal values of the parameters used for the fit of Figs. 5 and 6 are not the only optimal ones as, due to the fact that real data are used, there exists a neighborhood of optimal parameter values (see Section 5.3.2) for which the model fit provides a value of the cost function within the maximum levels.

The success of the application of ALOPEX IV optimization is, in these figures, evident.

6. Conclusion

We have demonstrated the successful application of the ALOPEX IV stochastic optimization method to the problem of optimal calculation of the parameters of the dynamical system model of the heart rate response to exercise, presented in [10, 25], for a particular subject.

The optimization method of ALOPEX IV is a very fast, easy to implement and efficient way to obtain the optimal parameters of the model that, as described in this paper, characterize the condition of the particular athlete. For the subject used in our study, the optimization revealed the optimal parameter neighborhood $0.45 < A < 0.65$, $1.55 < B < 1.75$, $1.60 < C < 1.80$.

It should be noted that the optimization method presented in this paper is not restricted to the calculation of the optimal parameter values of the model of the heart rate response to exercise [25], but can also be successfully applied to provide the optimal parameter values of a model describing the oxygen uptake kinetics [1]. In both these models, with the use of ALOPEX IV while fitting the models throughout training, it becomes very easy to track changes in the value of the parameters and subsequently important changes in the fitness level of the athlete.

Acknowledgements

This work was supported by the Program Ramon y Cajal 2004, Spanish Ministry of Science and Technology.

References

[1] J.R. Stirling, M.S. Zakynthinaki, B. Saltin, Bull. Math. Biol. 67 (5) (2005) 989.

[2] E. Harth, E. Tzanakou, Vision Res. 14 (1974) 1475.
[3] T. Tzanakou, R. Michalak, E. Harth, Biol. Cybern. 35 (1979) 161.
[4] T. Kalogeropoulos, Y.G. Saridakis, M.S. Zakynthinaki, Comput. Phys. Comm. 99 (1997) 255.
[5] Y.G. Saridakis, M.S. Zakynthinaki, T. Kalogeropoulos, Internat. J. Appl. Sci. Comp. 5 (3) (1999) 252.
[6] Y.G. Saridakis, M.S. Zakynthinaki, in: 3rd HERMIS Conference Proceedings, LEA, 1996, p. 251.
[7] M.S. Zakynthinaki, Stochastic optimization for adaptive correction of atmospheric distortion in astronomical observation, PhD thesis, Technical University of Crete, 2001.
[8] M.S. Zakynthinaki, Y.G. Saridakis, Comput. Phys. Comm. 150 (3) (2003) 274.
[9] M.S. Zakynthinaki, Y.G. Saridakis, Numer. Algorithms 33 (1) (2003) 509.
[10] J.R. Stirling, M.S. Zakynthinaki, Mathematical modeling in sport, in: Matematiques del segle XXI: dels fonaments a la tecnologia, III Cicle Ferran Sunyer i Balaguer, Fundacio Caixa de Sabadell, Barcelona, 2003, pp. 73–97.
[11] J.H. Wilmore, D.L. Costill, Physiology of Sport and Exercise, second ed., Human Kinetics, 1999.
[12] D.E. Martin, P.N. Coe, Better Training for Distance Runners, Human Kinetics, 1997.
[13] G.A. Brooks, T.D. Fahey, T.P. White, K.M. Baldwin, Exercise Physiology: Human Bioenergetics and its Applications, third ed., McGraw-Hill, 1999.
[14] E.R. Burke, Precision Heart Rate Training, Human Kinetics, 1998.
[15] S. Edwards, The Heart Rate Monitor Guidebook to Heart Zone Training, Performance Matters Pty Ltd, 1999.
[16] P.O. Åstrand, K. Rodahl, H.A. Dahl, S.B. Strømme, Textbook of Work Physiology—Physiological Bases of Exercise, fourth ed., Human Kinetics, 2003.
[17] M. Hitchen, D.A. Brodie, J.B. Harness, Ergonomics 23 (1980) 379.
[18] J. Daniels, Daniels' Running Formula, Human Kinetics, 1998.
[19] P. Maffetone, M.E. Mantell, The High Perfomance Heart, MBI Publishing Company, 1994.
[20] T. Noakes, Lore of Running. Discover the Science and Spirit of Running, Human Kinetics, 1991.
[21] B.A. Franklin, T. Noakes, O.A. Brusis, Active Cardiac Rehabilitation, Polar Electro Oy, 2001.
[22] J. Rippe, Target your Fitness and Weight Management Goals, Polar Electro Oy, 2000.
[23] K. Kukkonen-Harjula, R. Laukkanen, Precision Weight Management, Polar Electro Oy, 1998.
[24] K. Wasserman, J.E. Hansen, D.Y. Sue, R. Casaburi, B.J. Whipp, Principles of Exercise Testing and Interpretation, Including Pathophysiology and Clinical Applications, third ed., Lippincott Williams and Wilkins, 1999.
[25] J.R. Stirling, M.S. Zakynthinaki, Bull. Math. Biol. (2006), submitted for publication.
[26] B. Saltin, The physiological and biochemical basis of aerobic and anaerobic capacities in man; effect of training and range of adaption, in: An Update in Sports Medicine, Proc. 2nd Scandinavian Conference in Sports Medicine, 1987, p. 16.
[27] B. Saltin, Anaerobic capacity: Past, present and prospective, in: Biochemistry of Exercise VII, Human Kinetics, 1990, p. 387.
[28] J. Bangsbo, Sports Med. 22 (5) (1996) 299.
[29] V.L. Billat, E. Wesfreid, F. Cottin, C. Kapfer, J.-P. Koralsztein, S. Bonneau, Y. Meyer, Internat. J. Comp. Sci. in Sport 2 (2) (2003) 16.
[30] A.L. Goldberger, L.A.N. Amaral, J.M. Hausdorff, P.C. Ivanov, C.-K. Peng, H.E. Stanley, Proc. Natl. Acad. Sci. USA 99 (1) (2002) 2466.
[31] D. Linnarsson, Acta Physiol. Scand. 415 (Suppl.) (1974) 1.
[32] Polar, S625x Heart Rate Monitor, User Guide, Polar Electro Oy, 2004.
[33] Polar, S810i Heart Rate Monitor, User Guide, Polar Electro Oy, 2005.
[34] F.R. Borrani, G.Y. Canadau, S. Millet, J. Perrey, J. Fuchslocher, J.D. Rouillon, J. Appl. Physiol. 90 (2001) 2212.
[35] S.E. Bearden, R.J. Moffatt, J. Appl. Physiol. 88 (2000) 1407.
[36] A. Krogh, J. Lindhard, J. Physiol. 47 (1913) 112.
[37] D.C. Poole, G.A. Gaesser, M.C. Hogan, D.R. Knight, P.D. Wagner, J. Appl. Physiol. 72 (1992) 805.
[38] H.B. Rossiter, S.A. Ward, V.L. Doyle, F.A. Howe, J.R. Griffiths, B.J. Whipp, J. Physiol. 518 (1999) 921.
[39] G.A. Gaesser, D.C. Poole, Exerc. Sport Sci. Rev. 24 (1996) 35.
[40] D.C. Poole, Med. Sci. Sport Exerc. 26 (11) (1994) 1335.
[41] D.C. Poole, T.J. Barstow, G.A. Gaesser, W.T. Willis, B.J. Whipp, Med. Sci. Sport Exerc. 26 (11) (1994) 1354.
[42] B.J. Whipp, H.B. Rossiter, S.A. Ward, Biochem. Soc. Trans. 30 (2) (2002) 237.
[43] S.E. Bearden, P.C. Henning, T.A. Bearden, R.J. Moffatt, Eur. J. Appl. Physiol. 91 (2004) 586.
[44] J.R. Stirling, M.S. Zakynthinaki, V. Billat, Bull. Math. Biol. (2006), submitted for publication.
[45] E. Harth, Biol. Cybern. 22 (1976) 169.
[46] W.H. Press, S.A. Teukolsky, W.T. Vetterling, B.P. Flannery, Numerical Recipes, in C: The Art of Scientific Computing, second ed., Cambridge University Press, 1993.
[47] S.K. Mitra, Digital Signal Processing: A Computer-Based Approach, third ed., McGraw-Hill, 2006.
[48] J.G. Proakis, D.G. Manolakis, Digital Signal Processing: Principles, Algorithms and Applications, second ed., MacMillan Publishing Company, 1992.
[49] Garmin, Garmin Forerunner 201, Personal Trainer and Owner's Manual, Garmin Ltd., 2005.
[50] J. Karvonen, S. Chwalbinska-Moneta, Phys. Sport Med. 12 (6) (1984) 65.
[51] B. Seaward, R. Sleamaker, T. McAuliffe, J. Clapp, Biomed. Instrum. Technol. 24 (1) (1990) 37.
[52] R. Godsen, T. Carroll, S. Stone, Med. Sci. Sports Exerc. 23 (4) (1991).
[53] I. Lamarra, B.J. Whipp, S.A. Ward, K. Wasserman, J. Appl. Physiol. 62 (1987) 2003.
[54] F. Özyener, H.B. Rossiter, S.A. Ward, B.J. Whipp, J. Appl. Physiol. 53 (3) (2001) 891.
[55] H.B. Rossiter, F.A. Howe, S.A. Ward, J.M. Kowalchuk, J.R. Griffiths, B.J. Whipp, J. Physiol. 528 (2) (2000) 359.